PROCEEDINGS, 49th Workshop on Geothermal Reservoir Engineering
Stanford University, Stanford, California, February 12-14, 2024
SGP-TR-227

Coupled Hydro-Mechanical Back-Analysis of Circulation Program at FORGE in July of 2023

Zorica Radakovic-Guzina[1], Branko Damjanac[1], Wei Fu[1], Aleta Finnila[2], Rob Podgorney[3], John McLennan[4]

1 Itasca Consulting Group, Inc., Minneapolis, MN, USA

zorica@itascacg.com

2 WSP USA Inc., Redmond, WA, USA

aleta.finnila@wsp.com

3 Idaho National Laboratory, Idaho Falls, ID, USA

robert.podgorney@inl.gov

4 Department of Chemical Engineering, University of Utah, Salt Lake City, UT, USA

jmclennan@egi.utah.edu

Keywords: Circulation test, Utah FORGE, Enhanced Geothermal Systems (EGS), numerical modeling, lattice method, back-analysis.

ABSTRACT

In April of 2022, three stages of stimulation were carried out near the toe of well 16A(78)-32 at the Utah FORGE site. During the stimulations, pumping pressure, pumping rate, and microseismic events were recorded. The locations of microseismic events extended more than 100 m above well 16A(78)-32. Well 16B(78)-32 was drilled 100 m above the highly deviated lateral of well 16A(78)-32. In July of 2023, a circulation program was conducted between the two wells. The aim was to implement low-rate injection to interrogate the reservoir between the injection well and the production well, 16A(78)-32 and 16B(78)-32, respectively; assess the effect of reservoir stimulation in April of 2022; and determine the partitioning of flow between the three stimulation stages. Consequently, the circulation testing was designed to use low injection rates to limit the creation of new hydraulic fractures. Back analysis of the circulation test was carried out using a coupled hydro-mechanical model based on the discrete element method (DEM). The objective of the modeling was to interpret the state of the reservoir by matching the recorded injection pressures at well 16A(78)-32. The model includes an explicit representation of the discrete fracture network (DFN). Some DFN fractures were generated to match the observed microseismic event locations, while the majority were generated stochastically.

1. INTRODUCTION

Utah Frontier Observatory for Research in Geothermal Energy (FORGE) is an Enhanced Geothermal System (EGS) project supported by the U.S. Department of Energy. The drilling of injection well 16A(78)-32 was completed in December 2020. In April of 2022, three stages of reservoir stimulation by fluid injection were conducted at the toe of well 16A(78)-32 (McLennan et al., 2023). In June of 2023, production well 16B(78)-32 was drilled within the extent of the microseismic cloud recorded during the stimulation, 100 m above 16A(78)-32. In July of 2023, after drilling of the production well, circulation tests were conducted to assess the connectivity between wells 16A(78)-32 (injection) and 16B(78)-32 (production). The injection pressures recorded during the tests were back analyzed by different teams and using different methods, including analytical and different numerical modeling approaches. In this article, we present the back-analysis of injection pressures recorded during Day 1 (on July 4, 2023) Circulation Test 1 (two tests were carried out) using *XSite* (Itasca, 2020) with a thermo-hydro-mechanically coupled model based on the discrete element method (DEM) and lattice method. The objective of the back-analysis was to use the calibrated model (by matching the injection pressure history) to interpret the state of the reservoir near the toe of well 16A(78)-32 when the circulation tests commenced.

2. CIRCULATION TEST DATA

The circulation tests (including analysis of well connectivity) are discussed in detail by Xing et al. (2024) and only details of Day 1 of Circulation Test 1 relevant to the analysis described here are repeated. The geometry of the two wells and their completions at time of Circulation Test 1 are illustrated in Figure 1. Three stages were stimulated near the toe of well 16A(78)-32. Stage 1 of stimulation was conducted in the openhole section of the well, while Stages 2 and 3 were carried out through perforated sections in the well casing.

During the circulation tests, water was injected in all three stages along well 16A(78)-32. Recorded wellhead pressures for both wells and injection rates in 16A(78)-3 are shown in Figure 2. The injection started at 0.5 bpm, increased first to 2.5 bpm, and finally to a maximum rate of 5 bpm. The single pumping unit could not achieve 5 bpm at the wellhead pressure encountered, and a second (standby) unit was rigged up and brought online. Consequently, there were interruptions in the pumping and oscillations in both pumping rate and wellhead pressure.

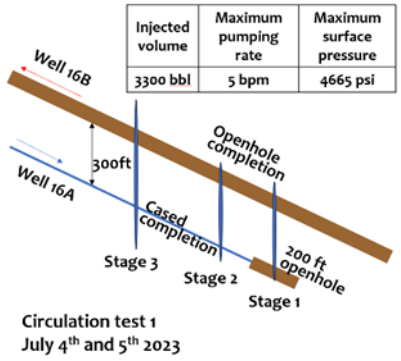

Figure 1: Illustration in vertical cross section of the well toe geometries and completions during Circulation Test 1 (after Xing et al. 2024).

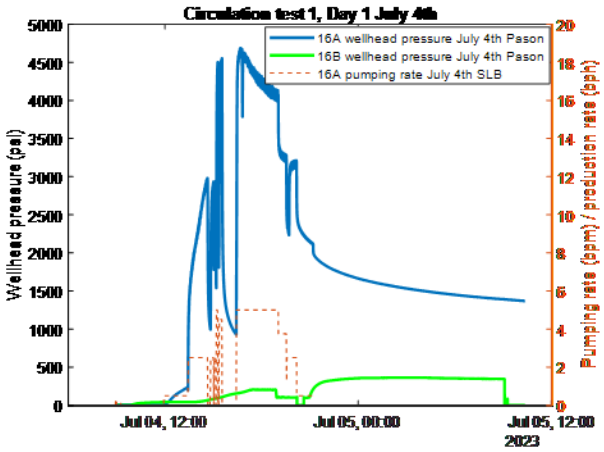

Figure 2: Wellhead pressure, injection rate, and producing rate during Day 1 of Circulation Test 1 (after Xing et al. 2024).

Well 16B(78)-32 produced fluid and recorded a pressure response (Figure **2**) during the first circulation test. About 40 minutes after initiation of injection, the pressure started to increase (relative to the initial value) in well 16B(78)-32. The wellhead pressure in well 16B(78)-32 built up slowly with the flow line closed (i.e., the well was shut-in at the surface and the throttling valve to the pit from the production well was closed). When the wellhead pressure in 16B(78)-32 reached 200 psi, the throttling valve in the flow line was opened to maintain 200 psi as back-pressure by flowing to the pit. Later during the pumping, the back pressure was reduced to 100 psi. After the injection stopped, both the injection well and the production well were shut in. The pressure in well 16B(78)-32 built up to a maximum of 362 psi.

3. DISCRETE FRACTURE NETWORK

Both the pre-existing natural fractures and new hydraulic fractures created during reservoir stimulation were explicitly represented in the model. Discrete stochastic fractures provided in the discrete fracture network (DFN) model have radii in the 10 to 150 m range and orientations matching the mean values of the four fracture sets identified from FMI logs (Finnila et al., 2021). The DFN was amended by adding fifteen fractures (shown in Figure 3) inferred by interpretation of the microseismic data recorded during the stimulation in 2022 (Finnila et al. 2023). Uncertainty in locations of the events recorded during stimulation of Stages 1 and 2 (and consequently in the geometry of the inferred fractures) is much greater than that for Stage 3 because during Stages 1 and 2, fewer, more distant geophones were used to record microseismicity.

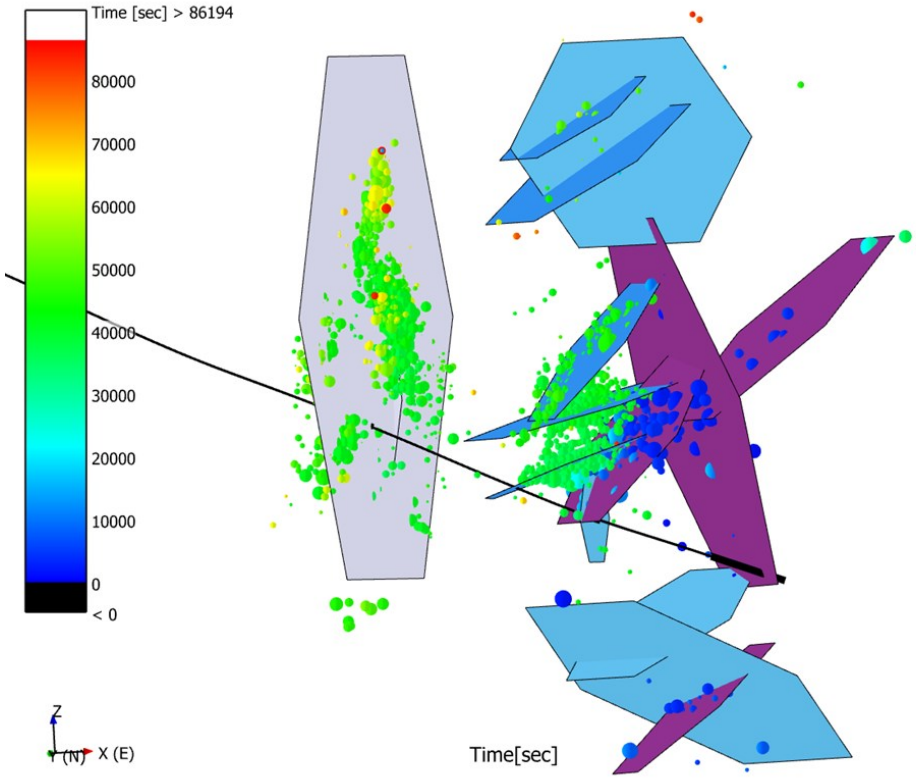

Figure 3. Geometry of the added fractures and the recorded microseismicity during reservoir stimulation in 2022. (The color scale indicates timing of the microseismic events relative to the beginning of injection.)

4. NUMERICAL MODEL

Day 1 of the Circulation Test 1 was simulated using the numerical code *XSite*, which implements the synthetic rock mass (SRM) model using the DEM and the lattice method (Damjanac et al. 2016). The model is fully coupled thermo-hydro-mechanically. The thermal processes were not simulated in these models because of the relatively short duration of the tests. In this model, deformation and damage of the reservoir rock mass include both the effects of deformation and damage of the intact rock (including hydraulic fracturing), and slip and opening of the pre-existing joints. Modeling of the circulation test using *XSite*, with the capability to approximate hydro-mechanical coupling, is important particularly during injection at higher rates (e.g., 2.5 bpm and 5 bpm), when the fluid pressures are expected to be sufficiently large to cause significant deformation of the fractures and change in their hydraulic apertures (i.e., permeability).

The material properties and initial stress conditions used by the numerical model are listed in Table 1. In the base case, it was assumed that the DFN, including the fractures created during stimulation, is frictional and permeable in-situ, which means that fluid can percolate through the DFN even before fractures fail either in shear or tension in response to stress changes induced by fluid injection during the circulation test. As shown in Table 2, DFN cohesion and tensile strength are assumed to be zero. The fracture permeability is based on the hydraulic apertures. After the excess pore pressures dissipated following the stimulation in 2022, the pore pressures returned to the initial hydrostatic state and the fractures closed, assuming that hydro-shearing and placed proppant volume were negligible. Although the fracture closed, it is assumed that there is a residual hydraulic aperture of 50 μm. In the base case, it was assumed that the entire DFN has the same mechanical and hydraulic properties.

The planned pumping schedule for Day 1 of Circulation Test 1 is shown in Figure 4. The rate oscillations that took place in the field were not reproduced in the model. In the model, fluid was injected at the (injection) points located at the intersections between well 16A(78)-32 and the fractures. No perforation pressure drop was considered for any of the injection points. The fluid is injected in all three stages simultaneously, and the code resolves distribution of the rate between the stages and injection points as a part of the model solution.

Table 1 Material properties and initial conditions for the circulation model with injection from well 16A(78)-32 (TVD 8490 ft, 2587.8 m).

Variable	Value
Young's modulus	55 GPa (8.0×10^6 psi)
Poisson's ratio	0.26
Fracture toughness	3 MPa×$m^{1/2}$ (2740 psi×$in^{1/2}$)
Fluid viscosity	Newtonian fluid, 2 cp
Pore pressure	0.0093 MPa/m (0.41 psi/ft), 24.0 MPa (3481 psi)
Minimum horizontal stress	0.0174 MPa/m (0.73 psi/ft), 42.68 MPa (6190 psi)
Maximum horizontal stress	0.0189 MPa/m (0.84 psi/ft), 48.80 MPa (7078 psi)
Vertical stress	0.0243 MPa/m (1.07 ft/ft), 62.80 MPa (9108 psi)

Table 2 Initial DFN properties used in the circulation model.

Parameter	Permeable and frictional DFN
DFN friction angle	37°
DFN cohesion	0
DFN tensile strength	0
Initial hydraulic aperture	50 μm

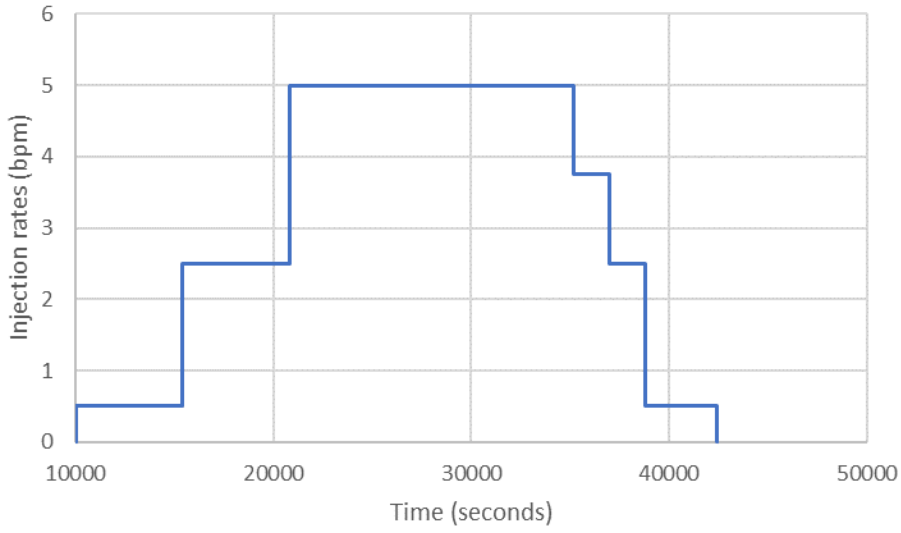

Figure 4. Simulated pumping schedule.

5. RESULTS

The contours of fracture fluid pressures and hydraulic apertures after seven hours of injection, obtained by the model for the base case, are shown in Figures 5 and 6, respectively. The plots illustrate the response governed by fluid pressure diffusion into a well-connected and permeable DFN at pressures smaller than the minimum stress (i.e., through closed but permeable DFN including fractures created during the 2022 stimulation). The increases in the hydraulic apertures, shown in Figure 6, of up to 0.5 mm indicate that although the fractures do not open, the hydro-mechanical coupling is important when injection rates increase to 2.5 and 5 bpm. The permeability of the reservoir at that stage is governed by the induced hydraulic aperture changes, not by the initial hydraulic apertures.

The downhole pressures calculated form the recorded surface pressures (using the approach presented by Xing et al. 2023) and obtained from the model are shown in Figure 7. The model results include pressure histories for all injection points. The difference between pressure histories for different injection points is mainly due to the hydrostatic pressure gradient and different depths. The base-case model does not match recorded pressures. At an injection rate of 0.5 bpm the model overpredicts the pressures; at greater rates, 2.5 and 5 bpm, the model underpredicts the recorded pressures. To investigate the effect of strength and permeability of the DFN, the sensitivity analysis was carried out assuming an impermeable DFN, cohesion and tensile strength of 0.1 MPa (in additional to the frictional shear strength component). The results obtained from such a model are shown in Figure 8. The model predictions of pressures during injection at 2.5 bpm are a better match of the field data. However, in this model the pressures during injection at 0.5 bpm are significantly overestimated.

Comparison of the results of two models with the field data indicate that during Day 1 of Circulation Test 1, the fully permeable and connected fracture network (i.e., stimulated reservoir volume) did not extend as far as the limits of the recorded microseismicity. On the other hand, there is a stimulated region around well 16A(78)-32 contained within the microseismic cloud. That stimulated region has initial permeability that allowed an injection at rate of 0.5 bpm without significant pressure increase (relative to the in-situ fluid pressure). That permeability should be greater than the equivalent permeability of the DFN with hydraulic aperture of 50 μm (assumed in the base case).

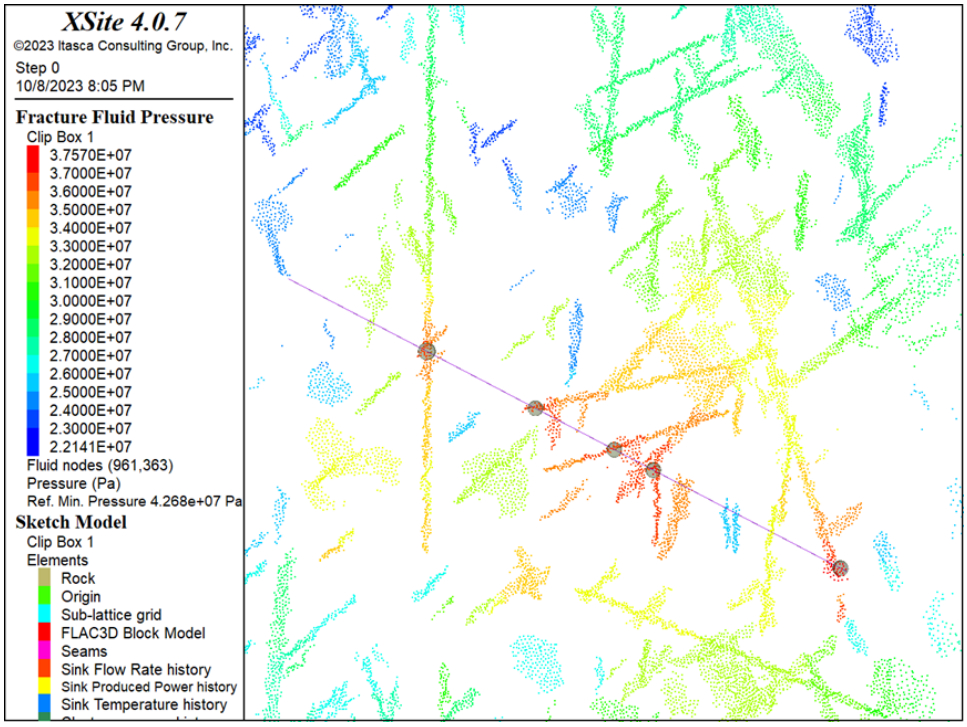

Figure 5. Fracture fluid pressure (Pa) contours after 7 hours of injection (before rate step down) in a vertical section along the sub-horizontal section of well 16A(78)-32. The well is shown as an inclined line segment and the injection points as spheres.

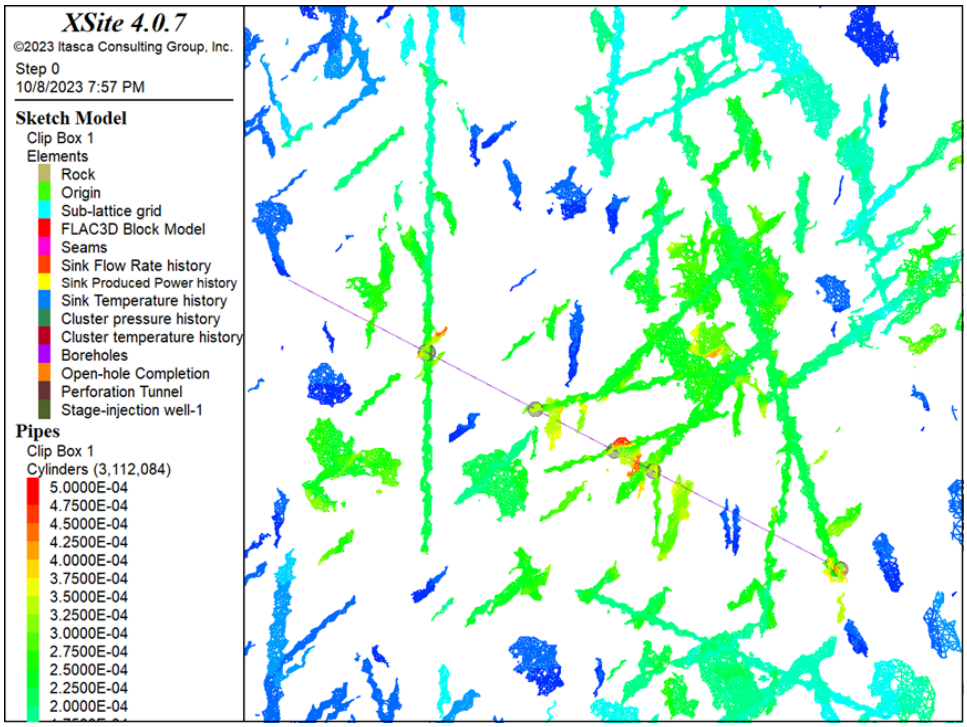

Figure 6. Fracture hydraulic aperture (m) contours after 7 hours of injection (before rate step down) in a vertical section along the sub-horizontal section of well 16A(78)-32. The well is shown as an inclined line segment and the injection points as spheres.

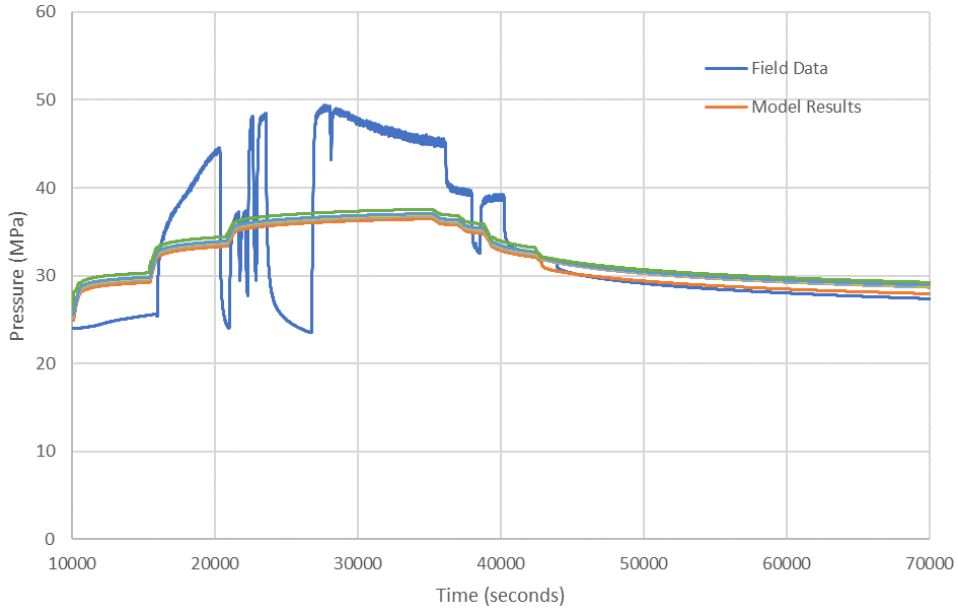

Figure 7. Comparison of the downhole pressure histories calculated from the field data and obtained from the base-case model which assumes an initially permeable, frictional DFN with initial hydraulic apertures of 50 µm.

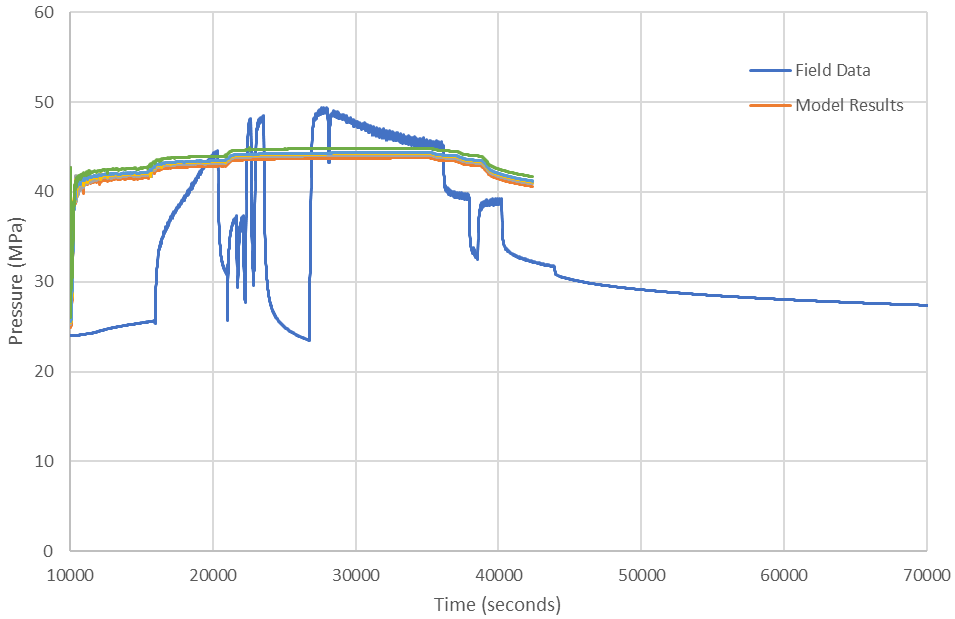

Figure 8. Comparison of the downhole pressure histories calculated from the field data and obtained from the model which assumes an initially impermeable DFN with initial hydraulic apertures of 50 µm and non-zero cohesive strength.

The model refined based on previous observations includes the initially permeable (stimulated) DFN within the 50-m radius around 16A(78)-32. Outside that radius the DFN is assumed to be impermeable with cohesion and tensile strength of 0.1 MPa in addition to the frictional resistance. The permeability and hydraulic apertures within the permeable part of the DFN are assumed to be variable depending on the distance from well 16A(78)-32. The extent of the permeable DFN and contours of the hydraulic aperture are shown in Figure 9. An initial hydraulic aperture of 0.2 mm is assumed within a radius of 25 m from well 16A(78)-32. The rest of the DFN within the permeable (stimulated) region is assumed to have hydraulic apertures of 0.1 mm.

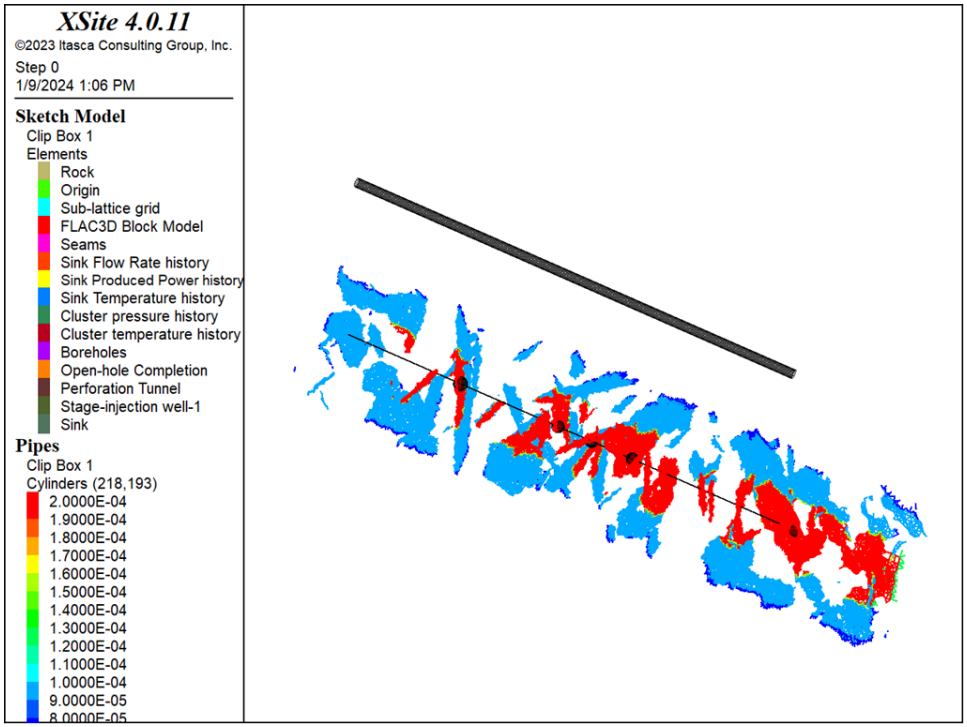

Figure 9. Initial hydraulic aperture (m) contours within the extent of initially permeable DFN (extending within 50 m radius from well 16A(78)-32) shown in a vertical cross-section along the sub-horizontal sections of two wells. The remaining DFN is impermeable and not shown in this plot. The wells are shown as inclined line segments (well 16A(78)-32 is shown as a thin line, well 16B(78)-32 as a cylindrical volume) and the injection points as spheres.

The downhole pressures obtained from the refined model compared with the pressures calculated using the recorded pressures are shown in Figure 10. This model better matches the pressures during 0.5 and 2.5 bpm injection rates, and the transition between the two. The pressure increases when the rate is increased from 2.5 to 5 bpm is not reproduced in the model well. A possible explanation for the mismatch at the 5 bpm rate is that the model includes the size of the inferred hydraulic fracture created during Stage 3 stimulation in 2022 with a radius of approximately 100 m. Thus, the model reopens the existing fracture perpendicular to the minimum horizontal principal stress beyond a radius of 50 m. In reality, that fracture probably extended (propagated) during Day 1 of Circulation Test 1, as microseismicity recorded at that time indicates. Reopening of the fracture underestimates the pressure, and the pressure history also does not exhibit the decaying trend observed from the recorded data.

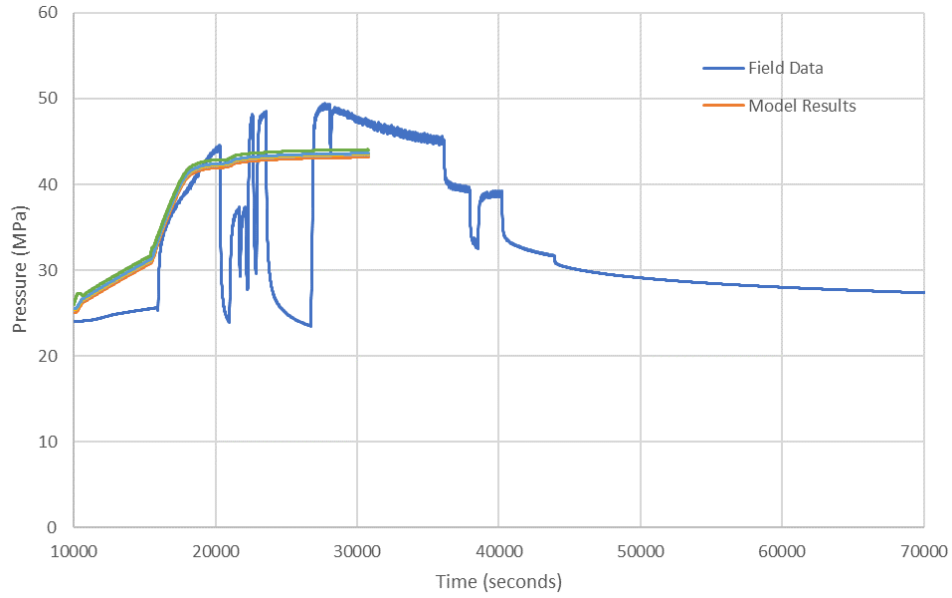

Figure 10. Comparison of the downhole pressure histories calculated from the field data and obtained from the base-case model which assumes initially heterogenous DFN permeability and strength.

6. DISCUSSION

The modeling results indicate that the stimulated reservoir volume (i.e., permeable and connected DFN) is smaller than the microseismic cloud. The injection pressure recorded during Day 1 of Circulation Test 1 and the results of the numerical model indicate that there is stimulated volume around well 16A(78)-32 with some residual permeability more than one year after stimulation. The extent of the domain with residual permeability is uncertain, but its radius around well 16A(78)-32 seems to be of the order of tens of meters. During injection at 0.5 bpm, fluid percolates into the permeable and connected DFN without significant pressure and permeability increase. At rates of 2.5 bpm the hydro-mechanical coupling becomes more dominant, causing hydraulic aperture changes greater than the initial apertures. Further increase of the rates to 5 bpm seems to result in fracture propagation. This model does not reproduce the fracture extension during the circulation test because the radius of the hydraulic fracture propagated during Stage 3 of the stimulation was overestimated in the model.

7. CONCLUSION

A fully coupled hydro-mechanical model with explicit representation of the DFN and capability to simulate hydraulic fracturing was used to back-analyze Day 1 of Circulation Test 1 conducted at the FORGE project in July of 2023. The recorded injection pressure history was used to calibrate the numerical model. Day 1 of Circulation Test 1 was conducted from well 16A(78)-32 by fluid injection at relatively low rates, between 0.5 and 5 bpm, simultaneously in all three stages stimulated in April of 2022. The objective of the numerical modeling was to use a calibrated model to better interpret the effect of stimulation on reservoir (or DFN) permeability more than one year after the stimulation was conducted.

The results of limited modeling study indicate that there is a domain around well 16A(78)-32 with increased residual permeability more than one year after the stimulation. Existence of such a domain is manifested by a relatively small pressure increase at an early time and small injection rate (0.5 bpm). The stimulated domain with increased permeability seems to be smaller than the extent of the microseismic cloud. Once the DFN was made impermeable outside a cylinder with a 50-m radius around well 16A(78)-32, the model was able to match the pressure increase when the rate was increased to 2.5 bpm. The model did not match further pressure increases when the rate was increased to 5 bpm because the size of the hydraulic fracture created during Stage 3 of the stimulation was overpredicted.

ACKNOWLEDGEMENTS

Funding for this work was provided by the U.S. DOE under grant DE-EE0007080 "Enhanced Geothermal System Concept Testing and Development at the Milford City, Utah FORGE Site." We thank the many stakeholders who are supporting this project, including Smithfield, Utah School and Institutional Trust Lands Administration, and Beaver County, as well as the Utah Governor's Office of Energy Development.

This research made use of the resources of the High Performance Computing Center at Idaho National Laboratory, which is supported by the Office of Nuclear Energy of the U.S. Department of Energy and the Nuclear Science User Facilities under Contract No. DE-AC07-05ID14517.

REFERENCES

Damjanac, B., Detournay, C. and Cundall, P. A. 2016. Application of particle and lattice codes to simulation of hydraulic fracturing. *Computational Particle Mechanics*, 3(2), 249–261. https://doi.org/10.1007/s40571-015-0085-0

Finnila, A., Doe, T., Podgorney, R., Damjanac, B., and Xing, P. 2021. Revisions to the Discrete Fracture Network Model at Utah FORGE Site, GRC Transactions, Vol. 45.

Finnila, A., Damjanac, B. and Podgorney, R. 2023. Development of a Discrete Fracture Network Model for Utah FORGE using Microseismic Data Collected During Stimulation of Well 16A(78)-32. In proceedings, 48th Workshop on Geothermal Reservoir Engineering, Stanford University, Stanford, California, February 6-8, 2023, SGP-TR-224.

Itasca Consulting Group, Inc. 2023. XSite (Version 4.0.07). Minneapolis: Itasca.

McLennan, J., England, K., Rose, P., Moore, J. and Barker, B. 2023. January. Stimulation of a High-Temperature Granitic Reservoir at the Utah FORGE Site. In SPE Hydraulic Fracturing Technology Conference and Exhibition. OnePetro.

Pengju X., Damjanac, B., Radakovic-Guzina, Z., Torres, M., Finnila, A., Podgorney, R., Moore, J., and McLennan, J. 2023. Comparison of Modeling Results with Data Recorded During Field Stimulations at Utah FORGE Site. In proceedings, 48th Workshop on Geothermal Reservoir Engineering, Stanford University, Stanford, California, February 6-8, 2023, SGP-TR-224.

Pengju X., England, K., Moore, J., Podgorney, R. and McLennan, J. 2024. January. Analysis of Circulation Tests and Well Connections at Utah FORGE. In proceedings, 49th Workshop on Geothermal Reservoir Engineering, Stanford University, Stanford, California, February 12-14, 2024, SGP-TR-227.